Bioorganic & Medicinal Chemistry Letters 19 (2009) 2492–2496

Contents lists available at ScienceDirect

Bioorganic & Medicinal Chemistry Letters

journal homepage: www.elsevier.com/locate/bmcl

1,5-Benzodiazepine inhibitors of HCV NS5B polymerase

David McGowan, Origène Nyanguile, Maxwell D. Cummings, Sandrine Vendeville, Koen Vandyck, Walter Van den Broeck, Carlo W. Boutton, Hendrik De Bondt, Ludo Quirynen, Katie Amssoms, Jean-François Bonfanti, Stefaan Last, Klara Rombauts, Abdellah Tahri, Lili Hu, Frédéric Delouvroy, Katrien Vermeiren, Geneviève Vandercruyssen, Liesbet Van der Helm, Erna Cleiren, Wendy Mostmans, Pedro Lory, Geert Pille, Kristof Van Emelen, Gregory Fanning, Frederik Pauwels, Tse-I Lin, Kenneth Simmen, Pierre Raboisson *

Tibotec BVBA, Gen. De Wittelaan L11 B3, B-2800 Mechelen, Belgium

ARTICLE INFO

Article history:
Received 20 January 2009
Revised 11 March 2009
Accepted 12 March 2009
Available online 14 March 2009

Keywords:
Hepatitis C virus
HCV
Polymerase
Benzodiazepine

ABSTRACT

Optimization through parallel synthesis of a novel series of hepatitis C virus (HCV) NS5B polymerase inhibitors led to the identification of (*R*)-11-(4-benzyloxy-2-fluorophenyl)-6-hydroxy-3,3-dimethyl-10-(6-methylpyridine-2-carbonyl)-2,3,4,5,10,11-hexahydro-dibenzo[*b*,*e*][1,4]diazepin-1-one **11zc** and (*R*)-11-(4-benzyloxy-2-fluorophenyl)-6-hydroxy-3,3-dimethyl-10-(2,5-dimethyloxazol-4-carbonyl)-2,3,4,5,10,11-hexahydro-dibenzo[*b*,*e*][1,4]diazepin-1-one **11zk** as potent (replicon EC_{50} = 400 nM and 270 nM, respectively) and selective (CC_{50} > 20 μM) inhibitors of HCV replication. These data warrant further lead-optimization efforts.

Approximately 170 million people (3% of the world population) are chronically infected by hepatitis C virus (HCV), a major cause of acute hepatitis and chronic liver disease.[1] Amongst all individuals contracting HCV, only 20% of them spontaneously clear the virus from their body, while the majority develops a chronic infection.[1] Untreated HCV infection can ultimately progress to cirrhosis, hepatocellular carcinoma, and liver failure.[2] As a result, HCV infection is the major indication for liver transplants in western countries.[2] Limited therapeutic options are currently available for patients infected with HCV: the current standard of care therapy consists of pegylated interferon-α combined with the broad spectrum antiviral drug ribavirin.[3] This treatment is often poorly tolerated due to side effects and is characterized by limited efficacy, especially when administered to patients infected with genotypes 1a and 1b, those most common in the European Union and the United States.[4] In this context, novel anti-HCV therapies directly targeting the virus life cycle will hopefully address this unmet medical need, by improving the efficacy and limiting the emergence of adverse events.

The RNA-dependent RNA polymerase (RdRp) NS5B is responsible for replication of the HCV genome. Intense drug discovery efforts directed toward the identification of potent and selective inhibitors of NS5B were initiated and have been subsequently validated in the clinic. These NS5B inhibitors can be divided into two distinct classes: nucleoside inhibitors (NIs) and non-nucleoside inhibitors (NNIs). NNIs can be further subdivided into at least four distinct families based on their respective binding pockets (NNI sites 1–4, Fig. 1).[5]

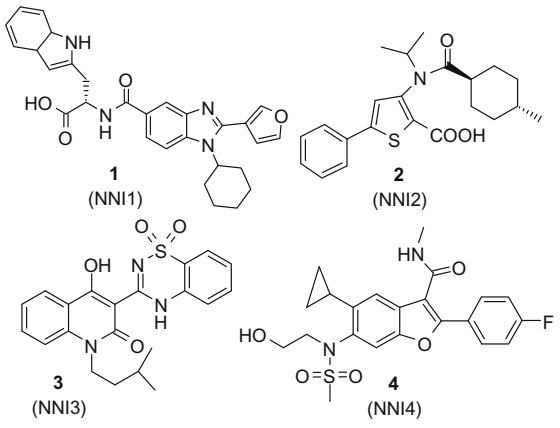

Figure 1. Representative examples of non-nucleoside HCV NS5B inhibitors and their respective binding pockets (NNI sites 1–4).[5]

* Corresponding author. Tel.: +32 15 44 42 62; fax: +32 15 40 12 57.
E-mail addresses: praboiss@its.jnj.com, PierreRaboisson@aol.com (P. Raboisson).

0960-894X/$ - see front matter © 2009 Elsevier Ltd. All rights reserved.
doi:10.1016/j.bmcl.2009.03.035

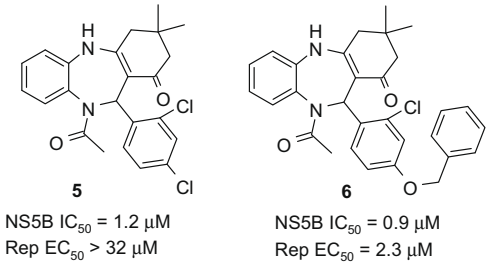

Figure 2. Previously reported 1,5-BZD HCV NS5B inhibitors.[6]

We have recently reported the discovery of the novel 1,5-benzodiazepine (1,5-BZD) HCV NS5B inhibitor **5** (Fig. 2), initially identified by high-throughput screening of a library of small molecules.[6] Herein we report our early lead optimization effort, using parallel synthesis, which led to the identification of submicromolar inhibitors of subgenomic replicons.

The 3-step parallel synthesis procedure[8] used for the synthesis of the target compounds **11a**–**zo** (Tables 1–3) is readily amenable to explore the structure–activity relationship (SAR) studies for this series of 1,5-BZDs at positions R^1, R^2, and R^3.

Condensation of aryldiamines **7a**–**i** with dimedone **8** in toluene at reflux afforded intermediates **9a**–**i** as major regioisomers, which were then condensed with aldehydes R^2CHO to form the 1,5-BZD **10a**–**x** in 12–65% yield. Intermediates **10a**–**x** were subsequently acylated using either an anhydride or an acyl chloride in the presence of diisopropylethylamine (DIPEA) to give final products **11a**–**c**, **11e**–**g**, and **11i** (Table 1). Noteworthy, when R^1 was a hydroxyl group, more than one acyl group (R^3CO–) was introduced on 1,5-BZD **10**. These undesired acyl functions were readily cleaved in basic conditions using a dilute solution of lithium hydroxide to afford the final products **11d**, **11h**, and **11j**–**zo** (Tables 1–3, 50–95% yield), each comprising a polysubstituted three-ring system (rings A, B and C, Scheme 1).

As shown in Table 1, preliminary SAR analysis both on ring A and on substituent R^2 was performed on a limited set of derivatives. Amongst the small substituents R^1 (compounds **11a**–**d**), the hydroxyl group was found to be of special interest, leading to a 31-fold improved activity (compare **5** to **11d**), as reported by us earlier.[6] Importantly, this activity was found to be highly stereodependent, since the (*R*)-enantiomer of **11d**, separated from (*S*)-**11d** by supercritical fluid chromatography (SFC), was found to be 178-fold more potent than (*S*)-**11d** (IC_{50} = 0.081 μM, and 14.4 μM, respectively).

With these encouraging results in hand, we decided to explore the effect of incorporation of nitrogen atoms in the A ring at positions X and Y. Although a nitrogen at position Y was found to be deleterious for activity (compare **11e** with **5**), its incorporation at position X (pyridine **11f**), or in both positions X and Y (pyrimidine **11g**), led to compounds with over 10-fold improved potency compared to **5**.[8] Surprisingly, and in contrast to the unsubstituted pyrimidine **11g** (IC_{50} = 0.51 μM), the corresponding 6-hydroxypyrimidine **11h** proved to be completely inactive (IC_{50} > 32 μM).

To help us understand our initial findings, and to guide our medicinal chemistry effort, the crystal structure of (*R*)-**11d** bound to HCV NS5B (NS5BΔC21, J4, genotype 1b)[5] was determined. Similar to the results of our previous work with a related compound of this chemotype,[6] (*R*)-**11d** was found to bind at the NNI3 binding site, adjacent to the polymerase active site (Fig. 3).[7] One face of the bound benzodiazepine fused ring system is solvent-exposed, while the dichlorophenyl ring is buried in a deep and largely hydrophobic pocket of NS5B. The hydroxyl group participates in an extensive network of intra- and intermolecular hydrogen bonds, partially mediated by bound water molecules and involving Ser367 and Tyr415 (Fig. 3). To our satisfaction, when the hydroxyl was introduced in the benzyloxy derivative **11i**, a very potent inhibitor **11j** was obtained (IC_{50} = 40 nM).

In an effort to improve the potency of the 1,5-BZD series, we analyzed the inhibitor-NS5B interactions of other chemotypes known to bind in the NNI-3 site (Figs. 1 and 4).[9] For example, superimposition of the NS5B-**13b** complex with that of **12**[6] shows extensive overlap of the phenoxy moiety of **13b**[9] and the benzyloxy group of **12** (Figs. 4 and 5).[6] We were able to exploit this particular 3D relationship to advance our lead optimization, although ultimately we found that the SAR of the acrylic acid series[9] was only partially transferable to the 1,5-BZDs. Although the introduction of the phenoxy moiety on the para position of the phenyl ring of **5**[6] conferred a ~20-fold increase in potency when compared to the dichlorophenyl derivative **5**[6] (IC_{50} = 3.1 μM and 0.16 μM, respectively for **5**[6] and **11k**), **11k** was found to be less potent than the corresponding benzyloxy derivative **11j**. Moreover, and in direct contrast to the 170-fold NS5B IC_{50} difference observed for acrylamide derivatives **13a** and **13b**,[9] the introduction of a bromo substituent at position 2 of the 1,5-BZD phenoxy ring gave a minimal 1.6-fold improvement in potency (IC_{50} = 0.16 μM and 0.10 μM

Table 1
SAR analysis on A ring and R^4 substituents

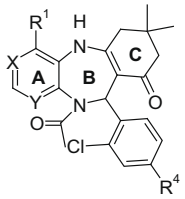

Compd #	X	Y	R^1	R^4	NS5B IC_{50} (μM)	HUH7-Rep EC_{50} (μM)
5[6]	CH	CH	H	Cl	3.1	>32
11a	CH	CH	CN	Cl	6.97	15.4
11b	CH	CH	Me	Cl	4.78	14.6
11c	CH	CH	Br	Cl	6.12	7.8
11d	CH	CH	OH	Cl	0.1	3
(*S*)-**11d**	CH	CH	OH	Cl	14.40	14.46
(*R*)-**11d**	CH	CH	OH	Cl	0.081	2.42
11e	CH	N	H	Cl	8.04	>32
11f	N	CH	H	Cl	0.51	>32
11g	N	N	H	Cl	0.51	>32
11h	N	N	OH	Cl	>32	>32
111[s]	CH	CH	H	OBn	0.90	2.3
11j	CH	CH	OH	OBn	0.04	1.5
11k	CH	CH	OH	OPh	0.16	9.9
11l	CH	CH	OH	O(2-Br)Ph	0.10	7.1
11m	CH	CH	OH	O(2-Br-6-F)Ph	0.12	6.3

Table 2
SAR analysis on R^2 susbstituent

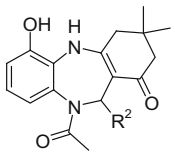

Compd #	R^2	NS5B IC_{50} (μM)	HUH7- Rep EC_{50} (μM)
11n	2-Furyl	21	43
11o	2-Pyridyl	>32	>32
11p	A/-Me-imidazol-2-yl	>32	>32
11q	A/-Me-indol-3-yl	13	>32
11r	5-OBn-2-thiophenyl-	0.18	11
11s	Cyclohexyl	22	0.74
11t	H	>32	>32

Table 3
SAR analysis on R^3 and R^4 position

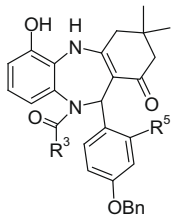

Compd#	R^3	R^5	NS5B IC_{50} (nM)	HUH7-Rep EC_{50}/CC_{50} (μM)
11j	CH_3	Cl	50	1.5/15
11u	*i*-Pr	Cl	154	1.5/17
11v	*i*-Pr	F	123	1.3/14
11w	*i*-Pr	Br	87	2.4/12
11x	*i*-Pr	CH_3	124	1.6/15
11y		F	51	0.36/15
11za		F	109	2.3/20
11zb		F	86	3.3/76
11zc	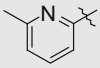	F	70	0.50/18
(*R*)- **11zc**	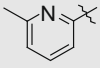	F	89	0.40/21
(*S*)- **11zc**	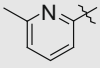	F	>11,000	5.7/18
11zd	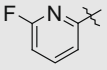	F	77	0.86/>32
11ze	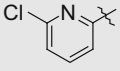	F	108	0.69/13
11f		F	75	2.2/16
11zg		F	111	1.7/19
11zh		F	39	0.76/29
11zi	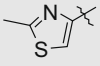	F	143	0.97/>32
11zj	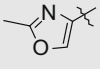	F	63	1.6/29

Table 3 (*continued*)

Compd#	R^3	R^5	NS5B IC_{50} (nM)	HUH7-Rep EC_{50}/CC_{50} (μM)
11zk	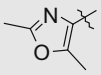	F	79	0.57/28
(*R*)-**11zk**	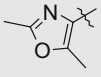	F	29	0.27/28
(*S*)-**11zk**	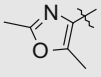	F	27,000	3.6/13
11zl	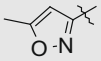	F	120	1.8/45
11zm	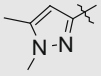	F	50	1.0/25
11zn		F	21	2.4/>32
11zo		F	60	0.73/>32

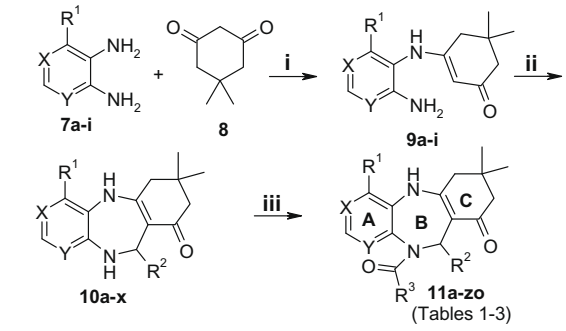

	X	Y	R^1
7a,**9a**	CH	CH	CN
7b,**9b**	CH	CH	CH_3
7c,**9c**	CH	CH	Br
7d,**9d**	CH	CH	OH
7e,**9e**	CH	CH	H
7f,**9f**	CH	N	H
7g,**9g**	N	CH	H
7h,**9h**	N	N	H
7i,**9i**	N	N	OH

	X	Y	R^1	R^2
10a	CH	CH	CN	2,4-diClPh
10b	CH	CH	CH_3	
10c	CH	CH	Br	
10d	CH	CH	OH	
10e	CH	N	H	
10f	N	CH	H	
10g	N	N	H	
10h	N	N	OH	
10i	CH	CH	H	4-(BnO)-2-ClPh
10j	CH	CH	OH	4-(BnO)-2-ClPh
10k	CH	CH	OH	4-(PhO)Ph
10l	CH	CH	OH	2-Br-4-(PhO)Ph
10m	CH	CH	OH	2-Br-6-F-4-(PhO)Ph
10n	CH	CH	OH	2-furyl
10o	CH	CH	OH	2-pyridyl
10p	CH	CH	OH	*N*-CH_3-imidazol-2-yl
10q	CH	CH	OH	*N*-CH_3-indol-3-yl
10r	CH	CH	OH	5-BnO-thiazol-2-yl
10s	CH	CH	OH	cyclohexyl
10t	CH	CH	OH	H
10u	CH	CH	OH	2-furyl
10v	CH	CH	OH	4-(BnO)-2-FPh
10w	CH	CH	OH	4-(BnO)-2-BrPh
10x	CH	CH	OH	4-(BnO)-2-CH_3Ph

Scheme 1. Reactions and conditions: (i) toluene reflux; (ii) R^2CHO, 10% acetic acid in ethanol 70 °C; (iii) acetic anhydride, reflux for **11a**–**t** or (a) R^3COCl, DIPEA, CH_2Cl_2 then for **11d**, **h**, **j**–**m**, **n**–**zo**; (b) LiOH, $MeOH/H_2O/THF$.

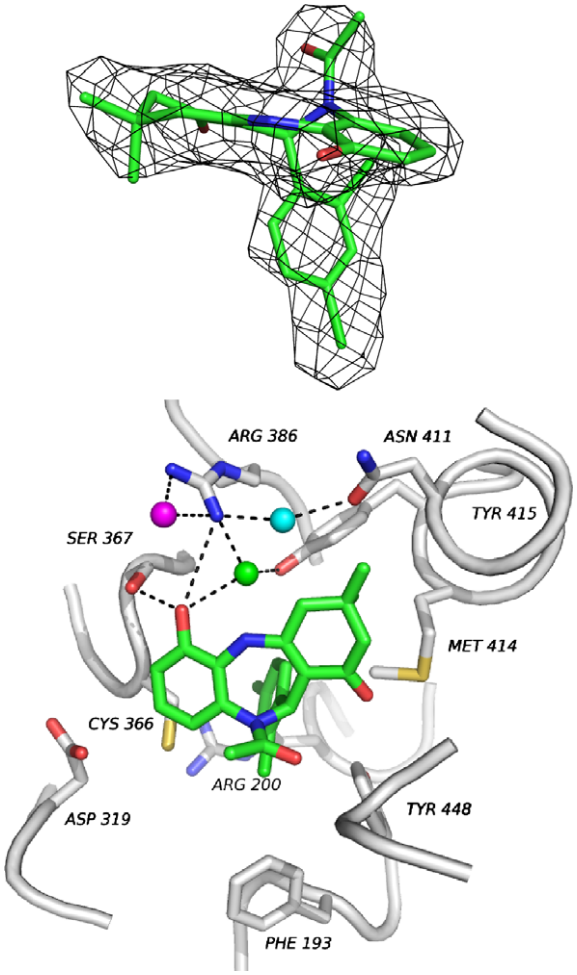

Figure 3. X-ray crystal structure of (*R*)-**11d** bound to HCV NS5B polymerase.[7] NS5B from monomer A of this structure is shown as white ribbon and white color-by-atom stick, and (*R*)-**11d** shown as green color-by-atom stick. *Upper*: the refined $2F_o - F_c$ electron density map of bound (*R*)-**11d** is contoured at 1σ. *Lower:* selected residues of the binding site showing a bound water from the A (cyan sphere) and B (magenta sphere) monomers of the asymmetric unit of this crystal structure, as well as one from another as yet unpublished structure from this series of inhibitors (green sphere).

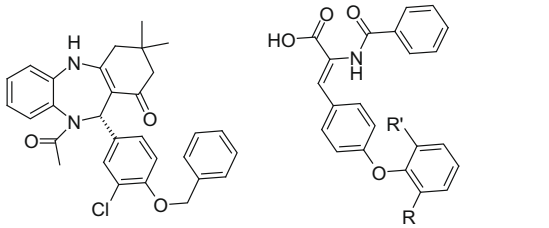

12[6]: IC_{50} = 1.0 μM

13a[9]: R = H, R' = H; IC_{50} = 17 μM*
13b[9]: R = Br, R' = H; IC_{50} = 0.10 μM*
13c[9]: R = Br, R' = F; IC_{50} = 0.03 μM*

Figure 4. Structure of previously reported 1,5-BZD **12**[6] and acrylic acid derivatives **13a–c**[9] and * reported IC_{50}.

for **11k** and **11l**, respectively). Finally, while in the acrylamide series the addition of an extra fluoro at position 6 of the phenoxy **13b** led to a further ~3-fold improvement (IC_{50} = 0.10 μM and 0.03 μM, respectively for **13b** and **13c**), similar modification of **11l** did not further improve the potency (**11m**-IC_{50} = 0.12 μM).

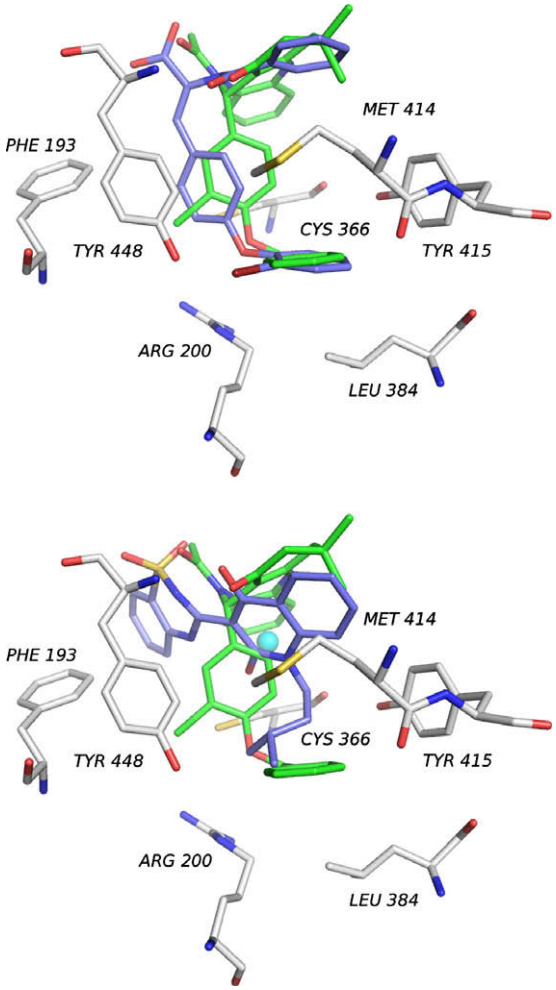

Figure 5. Superposition of the crystal structures of the NS5B complexes of **13b**[9] (upper panel; purple color-by-atom) and **3**[5] (lower; purple color-by-atom) onto **12** (green color-by-atom). Superposition was based on all common C_α of the two protein structures. Selected residues of NS5B from the complex with **12** are also shown. The cyan sphere in the lower panel depicts a bound water molecule from the crystal structure of **3**[5] displaced by the phenyl ring of NS5b-bound **12**.

Attempts to replace the benzyloxyphenyl moiety of **11j** with a cyclohexyl (**11s**) or with a mono- (**11n** and **11o**) or di-heteroaromatic ring systems (**11p–r**) resulted in a loss in potency (Table 2). Moreover, the removal of the benzyloxyphenyl moiety led to a completely inactive compound **11t** (IC_{50} > 32 μM). Although the importance of the R^5 substituent was shown in our earlier communication,[6] replacement of the chloro (**11u**) with a fluoro (**11v**), bromo (**11x**) or methyl (**11w**) was found to be well tolerated, causing only minor differences on both replicon and enzymatic activity (Table 3). Since the fluoro atom was the smallest substituent required to maintain potency and was readily obtained from the common intermediate **10o**, we decided to pursue further SAR analysis around the R^3 substituent on a series of 4-benzyloxy-2-fluorophenyl derivatives (**11y–zo**, Table 3). X-ray structure analysis of **11d** bound to NS5B suggested that the acetyl moiety at position 10 ($R^3 = CH_3$) could be replaced by a larger substituent. Given that this position is close to the protein surface, we envisaged that the introduction of other R^3-acyl groups, readily introduced at the end of the synthesis, would lead to compounds with improved potency. Indeed, compared to the isopropyl analog (**11v**), the 2-pyridylcarbonyl moiety at position 10 (compound **11y**) was found to increase both the enzymatic and replicon activities by ~3-fold. Interestingly, the 3- and 4-pyridyl derivatives (**11za** and **11zb**, respec-

tively) were found to be 10-fold less potent against replicon, while the enzymatic effect was less than twofold. None of the small substituents tested in the alpha position of the 2-pyridyl moiety were found to positively impact the potency in either the biochemical or replicon assays (compare **11zc**, **11zd**, and **11ze** with **11y**). The results for the pyridyl series prompted us to evaluate other small heterocycles bearing either an oxygen (2-furyl, **11zf**) or a nitrogen atom (**11zg**–**zo**) at the alpha position.

Amongst the compounds synthesized, the dimethyloxazole derivative **11zk** was the most active of the series, exhibiting similar enzymatic and replicon potencies when compared to the more active pyridyl analogs **11y** and **11zc**. Separation of the two enantiomers of **11zc** and **11zk** led to two very potent inhibitors both in the biochemical (IC_{50} (*R*)-**11zc** = 89 nM, IC_{50} (*R*)-**11zk** = 29 nM) and the replicon assays (EC_{50} (*R*)-**11zc** = 400 nM, EC_{50} (*R*)-**11zk** = 270 nM). Noteworthy, the selectivity index was found to be over 50-fold for (*R*)-**11zc** and 100-fold for (*R*)-**11zk**. For these two compounds the (*S*)-enantiomers were essentially inactive on the enzyme ($IC_{50} > 10\ \mu M$), while the replicon activity was found to be more than one order of magnitude lower for the (*S*)- versus the (*R*)-enantiomers. Moreover, based on the high permeability coefficient P_{app} observed for both (*R*)-**11zc** and (*R*)-**11zk** on CACO-2 cells (P_{app} (A–B) = 11.6×10^{-6} and 10.9×10^{-6} cm/s, respectively), these compounds are predicted to be absorbed after oral administration. These preliminary results suggest to us that further lead optimization efforts are warranted to optimize the potency and selectivity index of this novel series of HCV NS5B inhibitors.

References and notes

1. Shepard, C. W.; Alter, M. J. *Lancet* **2005**, *5*, 524.
2. Willems, M.; Metselaar, H. J.; Tilanus, H. W.; Schalm, S. W.; De Man, R. A. *Transpl. Int.* **2002**, *15*, 61.
3. (a) Strader, D. B.; Wright, T.; Thomas, D. L; Seeff L. B. *Hepatology* **2004**, *39*, 1147.; (b) Dixit, N. M.; Layden-Almer, J. E.; Layden, T. J.; Perelson, A. S. *Nature* **2004**, *432*, 922; (c) Fried, M. W. et al *N. Engl. J. Med.* **2002**, *347*, 975.
4. Fried, M. W.; Peter, J.; Hoots, K.; Gaglio, P. J.; Talbut, D.; Davis, P. C.; Key, N. S.; White, G. C.; Lindblad, L.; Rickles, F. R.; Abshire, T. C. *Hepatology* **2002**, *36*, 967.
5. Pauwels, F.; Mostmans, W.; Quirynen, L.; van der Helm, L.; Boutton, C. W.; Cleiren, E.; Raboisson, P.; Surleraux, D.; Nyanguile, O.; Simmen, K. A. *J. Virol.* **2007**, *81*, 6909.
6. Nyanguile, O.; Pauwels, F.; Van den Broeck, W.; Boutton, C. W.; Quirynen, L.; Ivens, T.; Van der Helm, L.; Vandercruyssen, G.; Mostmans, W.; Delouvroy, F.; Dehertogh, P.; Cummings, M. D.; Bonfanti, J.-F.; Simmen, K. A.; Raboisson, P. *Antimicrob. Agents Chemother.* **2008**, *52*, 4420.
7. Coordinates for structure have been deposited at Protein Data Bank (www.rcsb.org) under file name 3GOL.
8. Cortés Cortés, E.; Valencia Cornejo, A. L.; Garcia-Mellado de Cortés, O. *J. Heterocycl. Chem.* **2007**, *44*, 183.
9. Pfefferkorn, J. A.; Greene, M. L.; Nugent, R. A.; Gross, R. J.; Mitchell, M. A.; Finzel, B. C.; Harris, M. S.; Wells, P. A.; Shelly, J. A.; Anstadt, R. A.; Kilkuskie, R. E.; Schwende, F. J.; Koptab, L. A. *Bioorg. Med. Chem. Lett.* **2005**, *15*, 2481.